Warburg effect enhanced by AKR1B10 promotes acquired resistance to pemetrexed in lung cancer-derived brain metastasis

Wenwen Liu
The Second Hospital of Dalian Medical University
Wenzhe Duan
The Second Hospital of Dalian Medical University
Shengkai Xia
The Second Hospital of Dalian Medical University
Yang Zhou
The Second Hospital of Dalian Medical University
Mengyi Tang
The Second Hospital of Dalian Medical University
Mingxin Xu
The Second Hospital of Dalian Medical University
Xinyu Li
The Second Hospital of Dalian Medical University
Qi Wang (wqdlmu@163.com)
Dalian Medical University https://orcid.org/0000-0003-2427-7234

Research Article

Keywords:

Posted Date: December 21st, 2022

DOI: https://doi.org/10.21203/rs.3.rs-2331831/v1

Abstract

Background

Pemetrexed (PEM), as a rare chemotherapeutic agent that can efficiently cross the blood-brain barrier, has profound implications for the treatment of patients with lung cancer brain metastasis (BM). However, resistance to PEM limits the therapeutic efficacy. Aldo-keto reductase family 1 B10 (AKR1B10) was recently found to be elevated in lung cancer BM. The link between AKR1B10 and BM-acquired PEM is unknown.

Methods

PEM drug-sensitivity was assessed in the preclinical BM model of PC9 lung adenocarcinoma cells and the BM cells with or without AKR1B10 interference *in vitro* and *in vivo.* Metabolic reprogramming of BM attributed to AKR1B10 was identified by chromatography-mass spectrometry (GC-MS) metabolomics, and the mechanism of how AKR1B10 mediates PEM chemoresistance via a way of modified metabolism was revealed by RNA sequencing as well as further molecular biology experimental approaches.

Results

The brain metastasis subpopulation (PC9-BrM3) showed obvious resistance to PEM compared to the parental PC9 cells and silencing AKR1B10 in BM cells could increase the PEM sensitivity *in vitro* and *in vivo*. Metabolic profiling revealed that AKR1B10 prominently facilitated the Warburg metabolism characterized by the overproduction of pyruvate and lactate. Glycolysis regulated by AKR1B10 is vital for the resistance of lung cancer BM cells to PEM. In mechanism, knockdown of AKR1B10 elicited inhibition of a series of glycolysis-related enzymes (LDHA, LDHB) at the transcriptional level. Besides, the Warburg effects enhanced by AKR1B10 constantly fueled phosphoinositide 3-kinase signaling, which was also helpful for the chemoresistance.

Conclusions

Our finding demonstrated that AKR1B10 promotes acquired PEM resistance in lung cancer BM, providing novel strategies to sensitize PEM response in the treatment of lung cancer patients suffering from BM.

Introduction

Brain metastasis (BM) is a malignant event leading to poor prognosis in non-small cell lung cancer (NSCLC) patients; the limited treatment modalities and poor treatment outcomes are the main factors contributing to its poor prognosis (median survival: 4–6 months)[1, 2]. The current common treatment

strategy for BM is a combination of applicable options including surgery, radiotherapy, chemotherapy, molecular targeted therapy and anti-angiogenic therapy[3]. Pemetrexed (PEM)-platinum, remains the first-line chemotherapy in patients with metastatic NSCLC[4]. Particularly, PEM exhibited a greater ability to penetrate the blood-brain barrier (BBB) among chemotherapy agents, indicating a powerful potential in the treatment of BM. However, the response rate is not as effective as expected in BM populations[5–7]. Therefore, it's important to investigate the intrinsic mechanisms that contribute to the unfavorable response to PEM in metastatic tumor cells.

Aldo-keto reductase family 1 B10 (AKR1B10) is a member of the aldo-keto reductase superfamily. Under physiological conditions, it is mainly expressed in the intestinal system and exerts a cyto-detoxification effect as a reductase to protect cells from carbonyl damage[8]. In the last decade, the prominent role of AKR1B10 in malignancies has received widespread attention[9]. Increasing evidences have indicated that AKR1B10 takes part in the acquirement of chemo-resistance in several cancers, including hepatocellular carcinoma(HCC)[10–12], gastrointestinal cancer[13] and lung cancer[12, 14]. Besides, we have reported that AKR1B10 was significantly overexpressed in a lung cancer cell line with high BM potential and in NSCLC patients with BM in our previous work[15]. However, whether there is any association between elevated AKR1B10 expression and poor PEM drug response in lung cancer BM is unknown.

In this study, we found that brain metastatic lung cancer cells develop an obvious resistance to PEM and AKR1B10 plays a vital role in this acquirement of PEM resistance. By conducting concomitant metabolomics and RNA-sequencing study in BM cells with or without AKR1B10 genetic silence, we further revealed the underlying mechanism that AKR1B10 facilitates the Warburg metabolism by regulating the transcription of glycolysis-related enzymes (LDHA and LDHB), which leads to the acquired PEM resistance.

Materials And Methods

Cells and reagents

The human lung cancer cell line PC9 was purchased from the Chinese Academy of Medical Sciences (Beijing, China). The highly brain metastatic derivative (PC9-BrM3) was constructed by planting the parental cells PC9 into immunodeficient mice in a way of left ventricular injection and metastatic cells were extracted from harvested brain metastases; these injection-isolation-expansion cycling operations were repeated three times as previously indicated[15]. All cells were routinely cultured in Roswell Park Memorial Institute medium-1640 (RPMI1640) supplemented with 10% fetal bovine serum (FBS), 100 U/mL penicillin and streptomycin (all these reagents were obtained from Gibco, Invitrogen, Inc, California, USA) and maintained in a humidified atmosphere with 5% CO2 at 37°C. Pemetrexed Disodium (MB1183), 2-Deoxy-d-glucose (2-DG, MB5453) were purchased from Meilunbio (Dalian, China).

Cell Viability And Colony Formation Assay

Cell viability was measured by Cell Counting Kit-8 (K1018, ApexBio, Houston, USA) following the manufacturer's instructions. For colony formation, cells were harvested and seeded in 6-well plates at a density of 1,000 cells per well. After 10-days culture, cell colonies were fixed with 4% paraformaldehyde (P1110, Solarbio, Beijing, China) for 10 minutes and stained with 1% crystal violet (G1062, Solarbio, Beijing, China) for 20 minutes.

Analysis Of Cell Apoptosis

Cell apoptosis was assessed by flow cytometry. Briefly, cells were labeled by Annexin V-APC and 7-AAD dual staining according to the manufacturer's instructions (E-CK-A218, Elabscience, Wuhan, China). Subsequently labeled cells were collected and analyzed using a Flow Cytometer (AccuriC6, BD Biosciences).

Rna Interference (Rnai) And Plasmid Design And Transfection

The AKR1B10-targeting shRNA and its negative control shRNA (shNC) constructed in the LV2 lentiviral vector, and lentiviral particles expressing luciferase infused shRNA were packaged in 293T cells (GenePharma, Suzhou, China). The sequences of shRNAs were 5'-CACGCATTGTTGAGAACAT – 3'(sh1) and 5'-GTGCCTATGTCTATCAGAA – 3' (sh2). The target sequences of AKR1B10 plasmid were referred to its genetic sequence in the PubMed (https://www.ncbi.nlm.nih.gov/gene). Transfection was carried out as directed by the manufacturer. The knockdown or overexpression efficiency was validated by western blot analysis.

Western Blot Analysis

Cell proteins was extracted by RIPA lysis buffer (Meilunbio, Dalian, China) containing a protease inhibitor cocktail and a phosphatase inhibitor cocktail (Sigma, USA). The concentration of protein was assessed using the BCA assay kit (Thermo Fisher Scientific Inc., USA). Protein lysates were then separated by sodium dodecyl sulfate-polyacrylamide gel electrophoresis (SDS-PAGE) and transferred onto nitrocellulose membranes (Millipore, Billerica, USA). The membranes were blocked and then incubated with primary antibodies against AKR1B10 (1:2,000; ab192865, Abcam, UK), LDHA(1:2,000, ab53488, Abcam, UK), LDHB (1:10,000; ab53292, Abcam, UK), PI3K (1:1,000 dilution; #4257, Cell Signaling Technology, USA), phospho-PI3K (1:1,000 dilution; #17366, Cell Signaling Technology, USA), AKT (1:1,000 dilution; #13038, Cell Signaling Technology, USA), phospho-AKT (1:1,000 dilution; #4060, Cell Signaling Technology, USA) and β-actin (1:10,000; 66009-1-Ig, Proteintech, USA). After washing with 0.05% Tris-buffered saline/Tween-20 (TBST), the corresponding secondary antibodies conjugated with horseradish peroxidase (1:5,000; Proteintech, USA) were further used. The ECL western blotting substrate (Tanon, China) was used to analyze the chemiluminescence of the blots. Protein expression was quantified by Image J software (National Institutes of Health, USA).

Animal Studies

This work was approved by the Animal Ethics Review Committee of Dalian Medical University (No.00122773). Female BALB-c-nu mice (4–6 weeks) were purchased from the Beijing Vital River Laboratory Animal Technology Co. Ltd., China. After anesthetizing with ketamine (100 mg/kg body weight; Sigma, Missouri, USA) and xylazine (10 mg/kg body weight; Sigma, Missouri, USA), 1 million PC9-BrM3 cells with or without AKR1B10 knockdown (shAKR1B10 or shNC) in 100 μL PBS were injected into the left ventricle of each mouse. Brain colonization was monitored *in vivo* by bioluminescence imaging (BLI) weekly. Briefly, mice were anesthetized and injected intraperitoneally with D-Luciferin (150 mg/kg body weight; Promega, Wisconsin, USA), images were acquired using an IVIS Spectrum Xenogen machine (PerkinElmer, Massachusetts, USA). The Living Image software (version 2.50) was used to analyze the bioluminescence images. Pemetrexed disodium administration (n = 3, 100mg/kg, once every 5 days, intraperitoneal injection) was initiated after confirmation of colonization and the brain metastases was monitored *in vivo* by BLI weekly for 4 weeks.

Metabolomics Analysis

GC-MS-based cell metabolic profiling was performed similarly as previously described[16, 17]. In brief, cells were harvested with 1 mL of methanol/water solution (4:1, v/v) and the lysates was subsequently lyophilized. The lyophilized samples were treated with oximation and silylation reactions before GC-MS analysis. Quality-control (QC) samples were prepared and pretreated as the samples. GC-MS analysis was performed using a GCMS-QP2010 plus system (Shimadzu, Kyoto, Japan) coupled with a DB-5 MS fused-silica capillary column (30 m × 0.25 mm × 0.25 μm, Agilent Technologies, Palo Alto, CA). 1 μL of samples was injected with a split ratio of 1:20. The linear velocity of carrier gas (Helium, 99.9995%, China) was set at 40 cm/s. The oven temperature was kept at 80°C for 1 minute and raised to 210°C at increment of 30°C/min, then to 320°C at increment of 20°C/min and kept for 4 minutes. An electron ionization source (EI, 70 eV) was used for ionization. The data acquisition started at 2.92 min with the mass scan range of 50–600 m/z and the event time of 0.2 sec. The temperatures of the inlet, the transfer line and the ion source were 320, 300 and 230°C, respectively. ChromTOF 4.43 (LECO, Saint Joseph, USA) and GC – MS browser (Shimadzu, Kyoto, Japan) software were used to identify and quantify the metabolic features. The intensity of metabolic features was normalized to the total peak areas of raw data from cell samples. The PLS-DA model was analyzed by SIMCA 14.1 (Umetrics, Umea, Sweden). Five-six replicates were set for each group as biological replicates.

Measurement Of Pyruvate And Lactate

Pyruvic Acid Colorimetric Assay Kit (E-BC-K130-M, Elabscience, Wuhan, China) and L-Lactic Acid Colorimetric Assay Kit (E-BC-K044-M, Elabscience, Wuhan, China) were used to assess the level of pyruvate and lactate in cell lysates as directed by manufacturer's instructions. Data were standardized by the corresponding protein concentration which was determined by BCA assay kit.

Rna-sequencing Analysis

This work was supported by the Novogene (Beijing, China) Co. Ltd. The main experimental procedures of RNA-sequencing analysis, which include RNA quantification and qualification, library preparation for transcriptome sequencing trypsin digestion, clustering and sequencing and data analysis, are presented in the Supplementary methods in detail.

Quantitative-polymerase Chain Reaction (Q-pcr)

Total RNA was extracted using the Trizol® reagent (Transgen biotech, China) and quantitated at OD_{260}nm. Total RNA (1.0 μg) was treated with RNase-free DNase I and reverse-transcribed into cDNA using random primers and Superscript II® retrotranscriptase (Transgen biotech, China). The resulting cDNAs were mixed with the SYBR PCR master mix (Transgen biotech, China) and run on the StepOnePlus Applied Biosystems Realtime PCR machine (Roche, Swiss). One cycle of a denaturing step (3 min at 95°C) was applied, which was followed by 40 cycles of amplification (12 s at 95°C, 30s at 62°C and 30s at 72°C), with fluorescence measured during the extension. Primers used in this study are as follows:

GAPDH

5'-CATGAGAAGTATGACAACAGCCT-3'(forward);

5'-AGTCCTTCCACGATACCAAAGT-3'(reverse);

LDHA

5'-AAGCGGTTGCAATCTGGATT-3'(forward);

5'-GAGACACCAGCAACATTCATTCC-3'(reverse);

LDHB

5'-GCTGCCATGGATGGATTTTG-3'(forward);

5'-CCATCTTATGCACTTCCTTCCAA-3'(reverse);

The relative quantification value of mRNA expression was calculated using the comparative CT ($^{\Delta\Delta}$CT) method and Step-OnePlus software v2.0.1 (Applied Biosystems, USA) with *GAPDH* as an internal control.

Statistical analysis

GraphPad Prism software 8.0 was used for statistical analysis. Quantitative data are presented as mean (± standard deviation) values from at least 3 independent experiments. Differences between two groups were assessed using the *t*-test.

Results

Highly brain metastatic lung cancer cells achieved prominent resistance to PEM.

The highly brain metastatic lung cancer cells PC9-BrM3, which were derived from the parental PC9 cells and exhibit high propensity for BM, were established by us in previous work[15]. We evaluated the PEM drug sensitivity in PC9 and its highly brain metastatic subpopulation PC9-BrM3 by treating these two groups of cells with pemetrexed disodium. The results of cell viability assay and colony formation assay indicated obvious PEM resistance of the highly brain metastatic PC9-BrM3 compared with the parental PC9 group (Fig. 1A-B). Annexin-V assay showed that the apoptotic cells induced by PEM were significantly decreased in PC9-BrM3 (Fig. 1C), revealing similar trends to those observed in the cell viability and colony formation assays. Together, the results indicated significant PEM chemotherapeutic resistance of the brain metastatic lung cancer cells, suggesting that the intrinsic acquired alterations in brain metastatic cells are the main cause of poor chemotherapy outcomes.

Suppression of AKR1B10 attenuated PEM-chemoresistance of BM cells in vitro **and** in vivo. Since our previous work had found that AKR1B10 was significantly elevated either in PC9-BrM3 cells or in tissue and serum samples of NSCLC patients with BM, we verified the potential association between up-regulated AKR1B10 protein expression and the observed acquired drug resistance of brain metastatic cells. AKR1B10 was silenced with two different shRNAs (sh1 and sh2) in PC9-BrM3 cells (Fig. 2A) and the PEM sensitivities were then evaluated *in vitro* and *in vivo.*

The results of cell viability assays, clonogenicity assays and cell apoptosis assays were similar and all indicated that suppression of AKR1B10 significantly enhanced the response of PC9-BrM3 to PEM (Fig. 2B-D). We further confirmed the effect of AKR1B10 on the PEM therapeutic response *in vivo*. PC9-BrM3 cells with or without AKR1B10 knockdown (BrM3-shAKR1B10 or BrM3-shNC) were implanted into nude mice by intracardiac injection respectively. Once the BM was confirmed, mice were administered with PEM weekly. The regular BLI analysis showed a consistent result with *in vitro* assays that BrM3-shAKR1B10 was remarkably sensitive to PEM *in vivo* (Fig. 2E). Collectively, these data indicated that inhibition of AKR1B10 rendered the brain metastatic cells more responsive to PEM.

Metabolic profiling revealed that AKR1B10 significantly augmented the Warburg effect.

Increasing studies have given solid evidence that proteases alter organism phenotype by reprogramming cellular metabolism[18, 19]. To explore the endogenous metabolic changes brought by AKR1B10 in brain metastatic cells, we performed metabolomics in PC9-BrM3 cells with or without AKR1B10 silence (BrM3-shNC/shAKR1B10), and parental PC9 cells with or without AKR1B10 overexpression and its parental cells (PC9-NC/OE). A typical total ion chromatogram of cell metabolic profile was presented (Fig.S1A). The relative standard deviation (RSD) distribution of QC samples determined a good data quality of the work (Fig. S1B). The partial least-squares discriminant analysis (PLS-DA) displayed significantly different global changes in metabolic profile in each cell group (Fig. 3A), indicating an obvious metabolic shifting caused by AKR1B10; the permutation test indicated the robustness of the model with no signs of

overfitting (Fig. 3B). Univariate analysis revealed different metabolites either in PC9-OE cells compared with PC9-NC cells, or in BrM3- shAKR1B10 cells compared with BrM3-shNC cells (Fig. 3C, Table S1). We found that the levels of lactate, the end product of glycolysis, were accompanied by changes in AKR1B10. To reveal the metabolic disturbance by AKR1B10, we analyzed the differential metabolic pathway and listed the enriched KEGG pathways by mapping the different metabolites between PC9-OE and PC9-NC cell groups (Fig. 3D-E). The results indicated that AKR1B10 significantly influenced the Warburg effect (aerobic glycolysis) in tumor cells. To visualize the influence on the Warburg effect caused by AKR1B10, the changes of differential products (glucose, phosphoenolpyruvate, pyruvate, lactate) involved in the glycolytic pathway was displayed respectively (Fig. 3F), indicating a hyperactive Warburg effect in lung cancer cells with AKR1B10 overexpressed. We further verified the intracellular levels of pyruvate and lactate by kits and the results were consistent with the metabolomics (Fig. 3G-H). In general, these data suggested that AKR1B10 remarkably facilitate the Warburg effect in lung cancer BM cells.

Akr1b10-mediated Pem Resistance Is Dependent On The Enhanced Effects On Anaerobic Glycolysis

Warburg effect has been regarded as a hallmark of cancer that can promotes tumor initiation and drug resistance[20, 21]. We investigated whether the glycolysis is essential for the AKR1B10-mediated obtainment of PEM resistance in lung cancer BM cells. As expected, we found that the glycolytic inhibitor 2-DG reduced the PEM resistance of BrM3 cells without AKR1B10 silence (BrM3-shNC), as the same effect as AKR1B10 silence (Fig. 4A-C). Importantly, the increased drug resistance in PC9 cells with AKR1B10 overexpression (PC9-OE) was significantly abolished with 2-DG treatment (Fig. 4D-F), evidenced by cell viability assays, clonogenicity assays and cell apoptosis assays. Collectively, these results suggested that the Warburg effect is involved in the regulation of PEM resistance by AKR1B10.

Rna-seq Identified That Akr1b10 Facilitate The Warburg Metabolism By Regulating The Expression Of Glycolytic Enzymes

To reveal the underlying mechanism that AKR1B10 facilitate the Warburg metabolism, we employed RNA-seq in PC9-BrM3 cells with or without AKR1B10 silence (BrM3-shNC/shAKR1B10). The Pearson correlation coefficient analysis indicated good reproducibility of RNA-seq data (Fig.S2A). We used the absolute values of log2FoldChange > 0.5 and padj < 0.05 as the screening criteria to identify differential genes, and then mapped and enriched the downregulated differential genes in KEGG pathways. The pathway of pyruvate metabolism, which contains the glycolytic metabolism from pyruvate to lactate, was found enriched in BrM3-shAKR1B10 group compared with BrM3-shNC (Fig. 5A). The exact differential genes enriched in the pyruvate metabolism were lactate dehydrogenases (LDHA, LDHB), which facilitates glycolytic process by preferentially converting pyruvate to lactate[22]. It was identified that AKR1B10 silence leads to the downregulation of lactate dehydrogenases (Fig. 5B-D), revealing the mechanism on the regulation of AKR1B10 on the Warburg metabolism. Besides, phosphoinositide 3-kinase (PI3K)

pathway, also as a key link modulates the multidrug resistance of cancers[23], was enriched in the BrM3-shAKR1B10 group compared with BrM3-shNC (Fig. 5A, S2B). Since a recent study notably defined the association between glycolysis and PI3K pathway that glycolysis constantly enhanced PI3K pathway to control T cell immunity[24], we confirmed the effects of glycolysis on PI3K in BrM3 cells by treating the cells with 2-DG. The results of western blotting showed that inhibition of glycolysis resulted in the significant suppression of PI3K pathway (Fig. 5E), suggesting the potential mechanism by which AKR1B10-enhanced glycolysis promotes chemoresistance in BM cells.

Discussion

BM is the leading cause of poor prognosis for NSCLC patients. Pemetrexed is one of the preferred agents in non-squamous NSCLC with BM[25, 26]; however, it displays limited therapeutic efficacy against BM due to drug resistance and the blood-brain barrier (BBB). Recent studies have shown that impaired BBB allows tumor cells to invade the brain parenchyma and form brain metastases[15, 27], which also means the barrier that prevents the entry of drugs is broken, supporting the possibility that intrinsic reprogramming of metastatic cells take an essential part in the development of chemoresistance. In the present work, we used the previously constructed highly brain metastatic lung cancer cells (PC9-BrM3) and confirmed the acquired resistance of brain metastatic cells to PEM compared to it parental PC9 cells, which give a reasonable explanation for the poor clinical response to chemotherapy in BM populations. Hence, it's necessary to explore the intrinsic factors causing the altered drug sensitivity of BM.

AKR1B10 is a member of the AR superfamily and identified as a novel protein in human hepatocellular carcinoma (HCC)[28]. In our recent study, we demonstrated for the first time that AKR1B10, a protein that has been reported to be associated with drug resistance in a variety of primary tumors, is significantly elevated in PC9-BrM3 cells and NSCLC BM patients[15]. Here we found that suppression of AKR1B10 significantly attenuated the acquired PEM resistance in PC9-BrM3 cells, suggesting that AKR1B10 plays an important role in mediating the PEM resistance in BM.

Metabolic reprogramming is a hallmark of malignancy. Recent work has demonstrated the complexity of metabolic reprogramming in tumor metastasis, where the metabolic properties and preferences of tumors alter during cancer progression, which produces different tumor characteristics, such as acquisition of drug resistance, between primary and metastatic cancers[29]. Our previous research employed metabolomics in lung cancer BM subpopulations (PC9-BrMs) and its parental PC9, revealing a greatly altered metabolic profile of BM cells[16]. In the course of these recognitions, we propose that metabolic reprogramming contributes to acquired drug resistance in BM. By profiling the metabolism alternations brought by AKR1B10, we confirmed that AKR1B10 promotes the PEM resistance by facilitating the Warburg effect (aerobic glycolysis). It is worth mentioning that the effect of AKR1B10 on tumor metabolic reprogramming displays significant heterogeneity. In breast cancer, $AKR1B10^{High}$ tumor cells, which are associated with an increased incidence of lung metastatic relapse, are characterized with reduced glycolytic capacity and dependency on glucose as fuel source but increased utilisation of fatty acid

oxidation (FAO)[30]. Similarly, a recent study claims that Fidarestat induces glycolysis of NK cells through decreasing AKR1B10 expression to inhibit hepatocellular carcinoma progression, especially lung metastasis[31]. Here we identified an opposing role of AKR1B10 in lung cancer derived brain metastatic cells that AKR1B10 presents a facilitative effect on anaerobic glycolysis. We speculate that there are differences in AKR1B10 related regulatory metabolic mechanisms in different tumors and cell types, as AKR1B10 has long been regarded to exhibit distinct effects in a variety of tumors[11, 32–35]. For lung and liver, which are characterized by a high level of oxidative stress and create a challenging microenvironment for metastatic tumor cells due to the high concentrations of oxygen and exposure to toxic compounds, increased AKR1B10 activity could serve to protect tumor cells from oxidative stress-induced damage which impair the FAO metabolism[36, 37], leading to the a rebalancing of cellular metabolism in glycolysis and fatty acids. Brain microenvironment, which is characterized by presence of BBB and high oxygen and glucose demands, shows a high level of specificity compared with other organs. It reasonable that tumor cells adapt different metabolic reprogramming in the face of different metastatic microenvironments. The metabolic regulatory heterogeneity of AKR1B10 for different tumors and in the face of specific metastatic microenvironments deserves to be further explored in future studies.

The Warburg effect is considered a metabolic hallmark in malignant tumors. It refers to the metabolic shift that tumor cells preferentially converting glucose to pyruvate (followed by lactate formation) rather than oxidative phosphorylation to meet the energy requirements under physiological oxygen conditions. It is characterized the accumulation of lactate which is the end product of glycolysis. The accumulated lactate is thought to drive tumor development, on the one hand, lactate leads to tumor acidosis which synergistically promotes tumor progress and resistance to antineoplastic drugs[38], on the other hand, the non-metabolic functions of lactate has been highlighted recently that lactate-derived lactylation of protein lysine residues serves as an epigenetic modification to facilitate tumor malignant behaviors[39–41]. The level of lactate dehydrogenases, which are key enzymes converting pyruvate to lactate, reflects the ability of malignant cells to metabolize pyruvate to lactate. Here we identified that AKR1B10 regulates the transcription of lactate dehydrogenases (LDH-A, LDH-B), clarifying the mechanism that AKR1B10 enhance the glycolysis metabolism in BM cells. Interestingly, in the case of lactate dehydrogenase activation by AKR1B10, the substrate pyruvate remained in a state of significant accumulation accompanied by high expression of AKR1B10, suggesting that AKR1B10 may be involved in the pyruvate synthesis and uptake pathway in addition to regulating the glycolytic process from pyruvate to lactate.

In summary, the present study reveals that elevated AKR1B10 enhances glycolysis through regulation of lactate dehydrogenases expression, inhibiting the susceptibility of lung cancer BM cells to PEM (Fig. 6). These findings outline the importance of AKR1B10 in the BM resistance to tumor therapy via a way of metabolic reprogramming. Therefore, adjuvant application of AKR1B10-targeted inhibitors might be a new strategy to overcome chemotherapy resistance in lung cancer BM.

Declarations

Ethics approval and consent to participate

The animal study is approved by the Animal Ethics Review Committee of Dalian Medical University (No.00122773).

Consent for publication

Not applicable.

Competing interests

The authors declare no competing interests.

Funding

This work was supported by a grant from the National Natural Science Foundation of China (No. 82103054, 81972916, 21906014 and 82027805) and Basic Research Project of Liaoning Province Education Department (LJKQZ2021106).

Author's contributions

W.L, W.D, and S.X designed, performed, and analyzed experiments, performed bioinformatic analyses, and contributed to writing the manuscript. Y.Z performed and analyzed the metabonomics. M.T provided protocols and technical input. M.X helps the cell culture. Q.W and X.L conceived and supervised the project, and revise the manuscript. All authors read and approved the submitted manuscript.

Acknowledgements

We appreciate the support of the Liaoning Lung Cancer Translational Medicine Center and the Dalian Respiratory Protection Engineering Center Laboratory.

Availability of data and material

RNA sequencing data has been deposited in NCBI GEO with accession number GSE211215. All other data are available from the corresponding author (Qi Wang) upon reasonable request.

References

1. Achrol AS, Rennert RC, Anders C, et al. Brain metastases. Nat Rev Dis Primers. 2019;5(1):5.
2. Steeg PS, Camphausen KA, Smith QR. Brain metastases as preventive and therapeutic targets. Nat Rev Cancer. 2011;11(5):352–63.
3. Shi Y, Sun Y, Yu J, et al. [China Experts Consensus on the Diagnosis and Treatment of Brain Metastases of Lung Cancer (2017 version)]. Zhongguo Fei Ai Za Zhi. 2017;20(1):1–13.

4. Gadgeel S, Rodríguez-Abreu D, Speranza G, et al. Updated Analysis From KEYNOTE-189: Pembrolizumab or Placebo Plus Pemetrexed and Platinum for Previously Untreated Metastatic Nonsquamous Non-Small-Cell Lung Cancer. J Clin Oncol. 2020;38(14):1505–17.
5. Schiller JH, Harrington D, Belani CP, et al. Comparison of four chemotherapy regimens for advanced non-small-cell lung cancer. N Engl J Med. 2002;346(2):92–8.
6. Bailon O, Chouahnia K, Augier A, et al. Upfront association of carboplatin plus pemetrexed in patients with brain metastases of lung adenocarcinoma. Neuro Oncol. 2012;14(4):491–5.
7. Barlesi F, Gervais R, Lena H, et al. Pemetrexed and cisplatin as first-line chemotherapy for advanced non-small-cell lung cancer (NSCLC) with asymptomatic inoperable brain metastases: a multicenter phase II trial (GFPC 07 – 01). Ann Oncol. 2011;22(11):2466–70.
8. Luo DX, Huang MC, Ma J, Gao Z, Liao DF, Cao D. Aldo-keto reductase family 1, member B10 is secreted through a lysosome-mediated non-classical pathway. Biochem J. 2011;438(1):71–80.
9. Banerjee S. Aldo Keto Reductases AKR1B1 and AKR1B10 in Cancer: Molecular Mechanisms and Signaling Networks. Adv Exp Med Biol. 2021;1347:65–82.
10. Cheng BY, Lau EY, Leung HW, et al. IRAK1 Augments Cancer Stemness and Drug Resistance via the AP-1/AKR1B10 Signaling Cascade in Hepatocellular Carcinoma. Cancer Res. 2018;78(9):2332–42.
11. Zhang T, Guan G, Zhang J, et al. E2F1-mediated AUF1 upregulation promotes HCC development and enhances drug resistance via stabilization of AKR1B10. Cancer Sci. 2022;113(4):1154–67.
12. Zhong L, Shen H, Huang C, Jing H, Cao D. AKR1B10 induces cell resistance to daunorubicin and idarubicin by reducing C13 ketonic group. Toxicol Appl Pharmacol. 2011;255(1):40–7.
13. Matsunaga T, Kawabata S, Yanagihara Y, et al. Pathophysiological roles of autophagy and aldo-keto reductases in development of doxorubicin resistance in gastrointestinal cancer cells. Chem Biol Interact. 2019;314:108839.
14. Endo S, Xia S, Suyama M, et al. Synthesis of Potent and Selective Inhibitors of Aldo-Keto Reductase 1B10 and Their Efficacy against Proliferation, Metastasis, and Cisplatin Resistance of Lung Cancer Cells. J Med Chem. 2017;60(20):8441–55.
15. Liu W, Song J, Du X, et al. AKR1B10 (Aldo-keto reductase family 1 B10) promotes brain metastasis of lung cancer cells in a multi-organ microfluidic chip model. Acta Biomater. 2019;91:195–208.
16. Liu W, Zhou Y, Duan W, et al. Glutathione peroxidase 4-dependent glutathione high-consumption drives acquired platinum chemoresistance in lung cancer-derived brain metastasis. Clin Transl Med. 2021;11(9):e517.
17. Zhou Y, Song R, Zhang Z, et al. The development of plasma pseudotargeted GC-MS metabolic profiling and its application in bladder cancer. Anal Bioanal Chem. 2016;408(24):6741–9.
18. Hochrein SM, Wu H, Eckstein M, et al. The glucose transporter GLUT3 controls T helper 17 cell responses through glycolytic-epigenetic reprogramming. Cell Metab. 2022;34(4):516–32.e11.
19. Martínez-Reyes I, Chandel NS. Cancer metabolism: looking forward. Nat Rev Cancer. 2021;21(10):669–80.

20. Ma L, Liu W, Xu A, et al. Activator of thyroid and retinoid receptor increases sorafenib resistance in hepatocellular carcinoma by facilitating the Warburg effect. Cancer Sci. 2020;111(6):2028–40.
21. Bhattacharya B, Mohd Omar MF, Soong R. The Warburg effect and drug resistance. Br J Pharmacol. 2016;173(6):970–9.
22. Huo N, Cong R, Sun ZJ, et al. STAT3/LINC00671 axis regulates papillary thyroid tumor growth and metastasis via LDHA-mediated glycolysis. Cell Death Dis. 2021;12(9):799.
23. Liu R, Chen Y, Liu G, et al. PI3K/AKT pathway as a key link modulates the multidrug resistance of cancers. Cell Death Dis. 2020;11(9):797.
24. Xu K, Yin N, Peng M, et al. Glycolysis fuels phosphoinositide 3-kinase signaling to bolster T cell immunity. Science. 2021;371(6527):405–10.
25. He G, Xiao X, Zou M, Zhang C, Xia S. Pemetrexed/cisplatin as first-line chemotherapy for advanced lung cancer with brain metastases: A case report and literature review. Med (Baltim). 2016;95(32):e4401.
26. Bearz A, Garassino I, Tiseo M, et al. Activity of Pemetrexed on brain metastases from Non-Small Cell Lung Cancer. Lung Cancer. 2010;68(2):264–8.
27. Li B, Wang C, Zhang Y, et al. Elevated PLGF contributes to small-cell lung cancer brain metastasis. Oncogene. 2013;32(24):2952–62.
28. Ye X, Li C, Zu X, et al. A Large-Scale Multicenter Study Validates Aldo-Keto Reductase Family 1 Member B10 as a Prevalent Serum Marker for Detection of Hepatocellular Carcinoma. Hepatology. 2019;69(6):2489–501.
29. Faubert B, Solmonson A, DeBerardinis RJ. Metabolic reprogramming and cancer progression. Science. 2020. 368(6487).
30. van Weverwijk A, Koundouros N, Iravani M, et al. Metabolic adaptability in metastatic breast cancer by AKR1B10-dependent balancing of glycolysis and fatty acid oxidation. Nat Commun. 2019;10(1):2698.
31. Wu T, Ke Y, Tang H, Liao C, Li J, Wang L. Fidarestat induces glycolysis of NK cells through decreasing AKR1B10 expression to inhibit hepatocellular carcinoma. Mol Ther Oncolytics. 2021;23:420–31.
32. Taskoparan B, Seza EG, Demirkol S, et al. Opposing roles of the aldo-keto reductases AKR1B1 and AKR1B10 in colorectal cancer. Cell Oncol (Dordr). 2017;40(6):563–78.
33. Yao Y, Wang X, Zhou D, et al. Loss of AKR1B10 promotes colorectal cancer cells proliferation and migration via regulating FGF1-dependent pathway. Aging. 2020;12(13):13059–75.
34. Shao X, Wu J, Yu S, Zhou Y, Zhou C. AKR1B10 inhibits the proliferation and migration of gastric cancer via regulating epithelial-mesenchymal transition. Aging. 2021;13(18):22298–314.
35. Endo S, Matsunaga T, Nishinaka T. The Role of AKR1B10 in Physiology and Pathophysiology. Metabolites. 2021. 11(6).
36. Schafer ZT, Grassian AR, Song L, et al. Antioxidant and oncogene rescue of metabolic defects caused by loss of matrix attachment. Nature. 2009;461(7260):109–13.

37. Carracedo A, Cantley LC, Pandolfi PP. Cancer metabolism: fatty acid oxidation in the limelight. Nat Rev Cancer. 2013;13(4):227–32.
38. Vaupel P, Schmidberger H, Mayer A. The Warburg effect: essential part of metabolic reprogramming and central contributor to cancer progression. Int J Radiat Biol. 2019;95(7):912–9.
39. Zhang D, Tang Z, Huang H, et al. Metabolic regulation of gene expression by histone lactylation. Nature. 2019;574(7779):575–80.
40. Yu J, Chai P, Xie M, et al. Histone lactylation drives oncogenesis by facilitating m(6)A reader protein YTHDF2 expression in ocular melanoma. Genome Biol. 2021;22(1):85.
41. Gu J, Zhou J, Chen Q, et al. Tumor metabolite lactate promotes tumorigenesis by modulating MOESIN lactylation and enhancing TGF-β signaling in regulatory T cells. Cell Rep. 2022;40(3):111122.

Figures

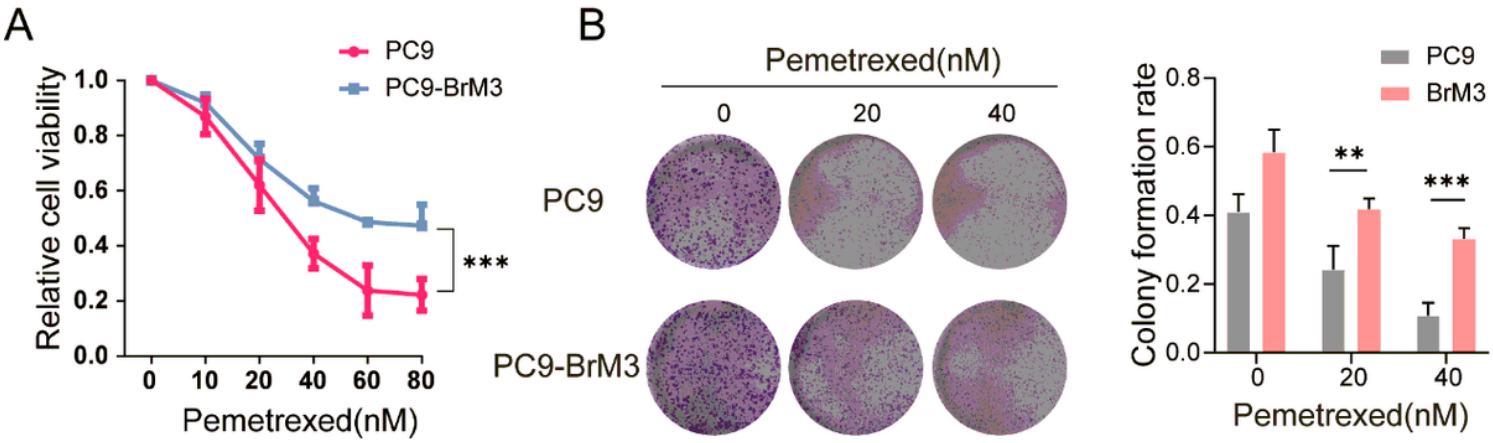

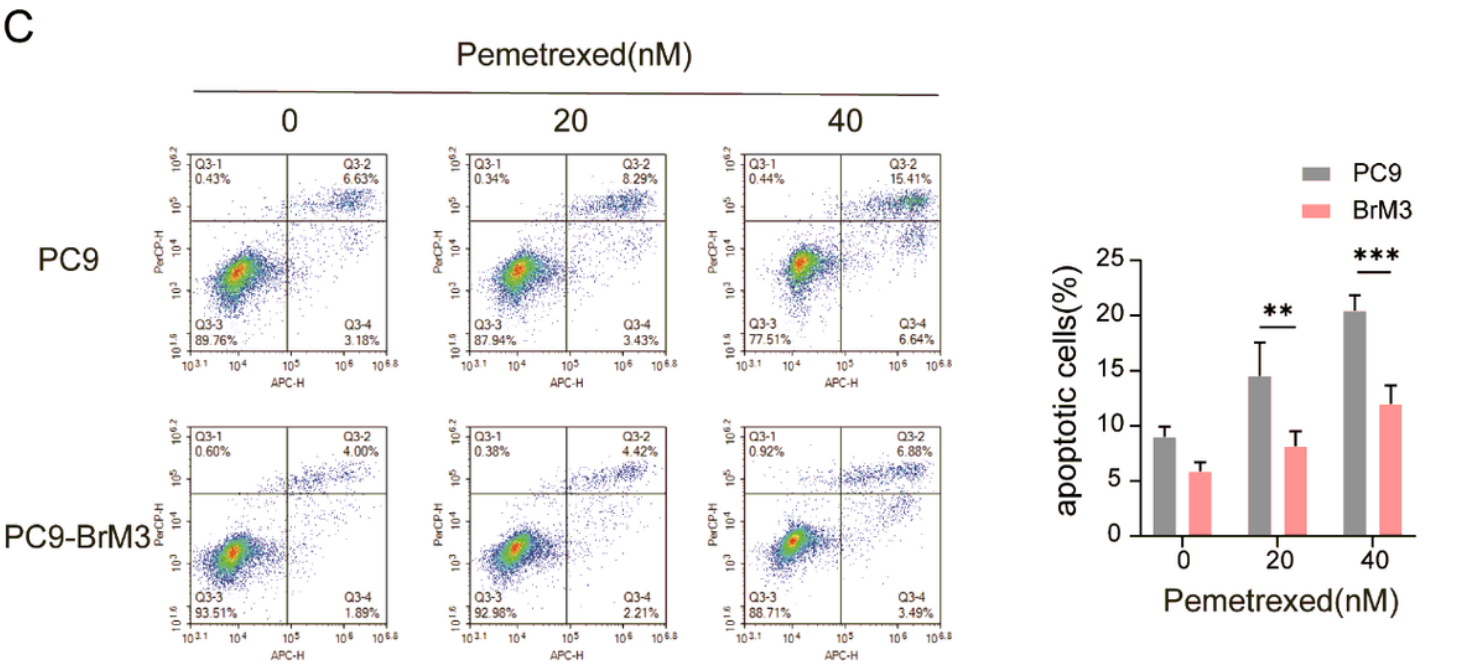

Figure 1

Highly brain metastatic lung cancer cells achieved prominent resistance to PEM. (A) PC9 and PC9-BrM3 cells were treated with different doses of PEM for 72 h and CCK-8 assays were performed to determine their viability. (B) Survival of PC9 and PC9-BrM3 cells after treatment with certain concentrations of PEM (0, 20, 40nM) and the results of clonogenic assays showing the treatment effect. Pixel density quantification of clonogenic assays is shown as histogram. (C) Flow cytometry analysis of PC9 and PC9-BrM3 cells treated with PEM (20nM) for 24h. (n=3, **p<0.01, ***p<0.001)

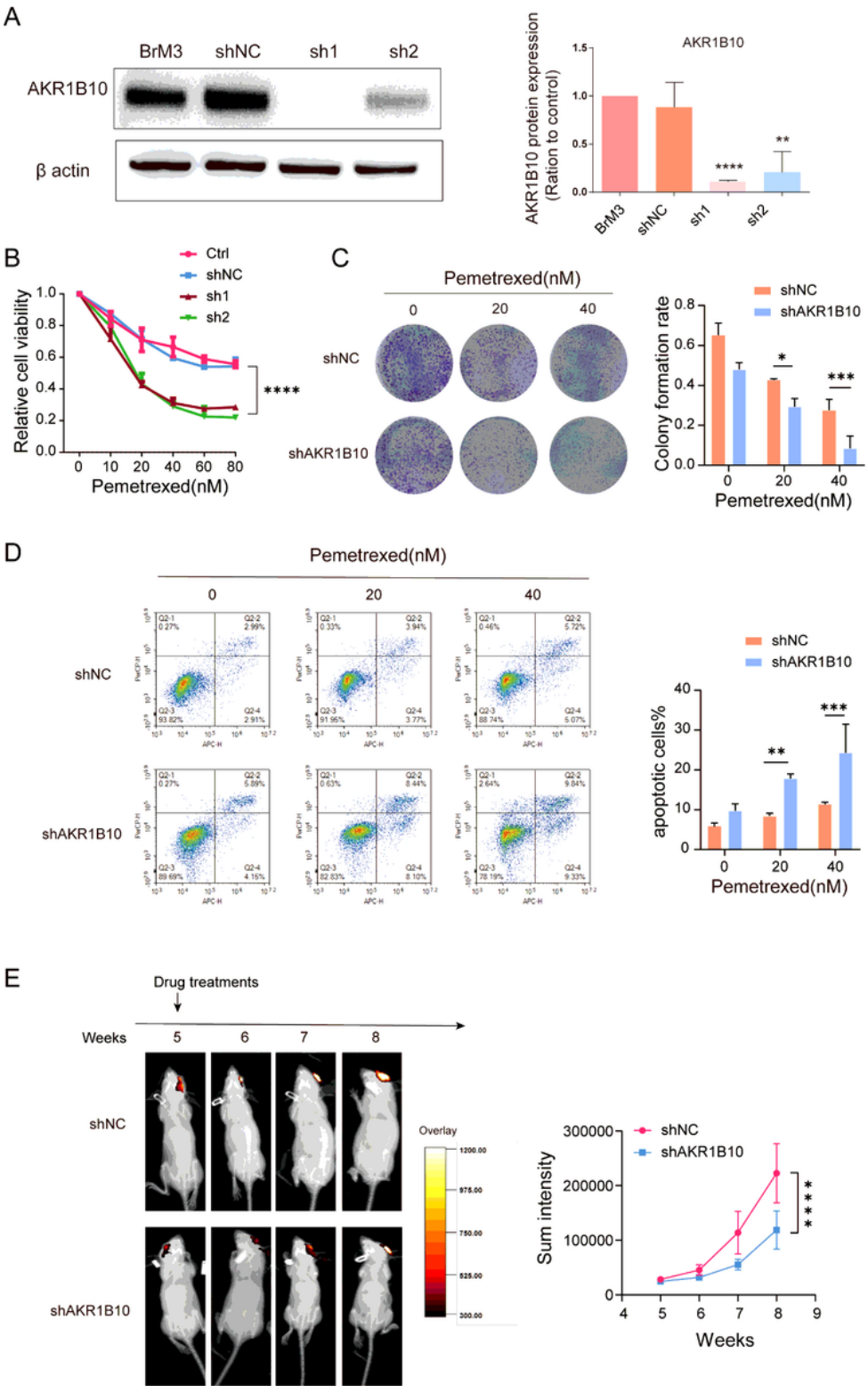

Figure 2

Suppression of AKR1B10 attenuated PEM-chemoresistance of BM cells *in vitro* and *in vivo*. (A) Western blotting showing the AKR1B10 knockdown efficiencies in PC9-BrM3 cells. (B) Indicated AKR1B10 knockdown PC9-BrM3 cells were treated with different doses of PEM for 72 h and CCK-8 assays were performed to determine their viability. (C) Results of clonogenic assays showing cell survival of the AKR1B10 knockdown PC9-BrM3 cells after treatment with certain concentrations of PEM (0, 20, 40 nM).

Pixel density quantification of clonogenic assays is shown as histogram. (D) Flow cytometry analysis of AKR1B10 knockdown PC9-BrM3 cells treated with PEM (20nM) for 24h. (E) Heat map image representations of bioluminescence intensity for representative mice from the indicated groups of the therapy response experiment. Nude mice were implanted with PC9-BrM3 cells with or without AKR1B10 knockdown (10^6 cells/mouse) by intracardiac injection. PEM Treatments (n=3, 100mg/kg, once a week, i.p.) were initiated at the 5th week. Bioluminescence intensity in the same bioluminescence heat map range was measured every week. Plot of mean bioluminescence readings for control and treatment group mice; the standard error is indicated for each imaging point. (n=3, **p<0.01, **p<0.0001, Ctrl, control PC9-BrM3 cells; shNC, PC9-BrM3 cells transfected with negative control shRNA; sh1, PC9-BrM3 cells transfected with AKR1B10-targeted shRNA vector 1; sh2, PC9-BrM3 cells transfected with AKR1B10-targeted shRNA vector 2; shAKR1B10, PC9-BrM3 cells transfected with AKR1B10-targeted shRNA vector 1)

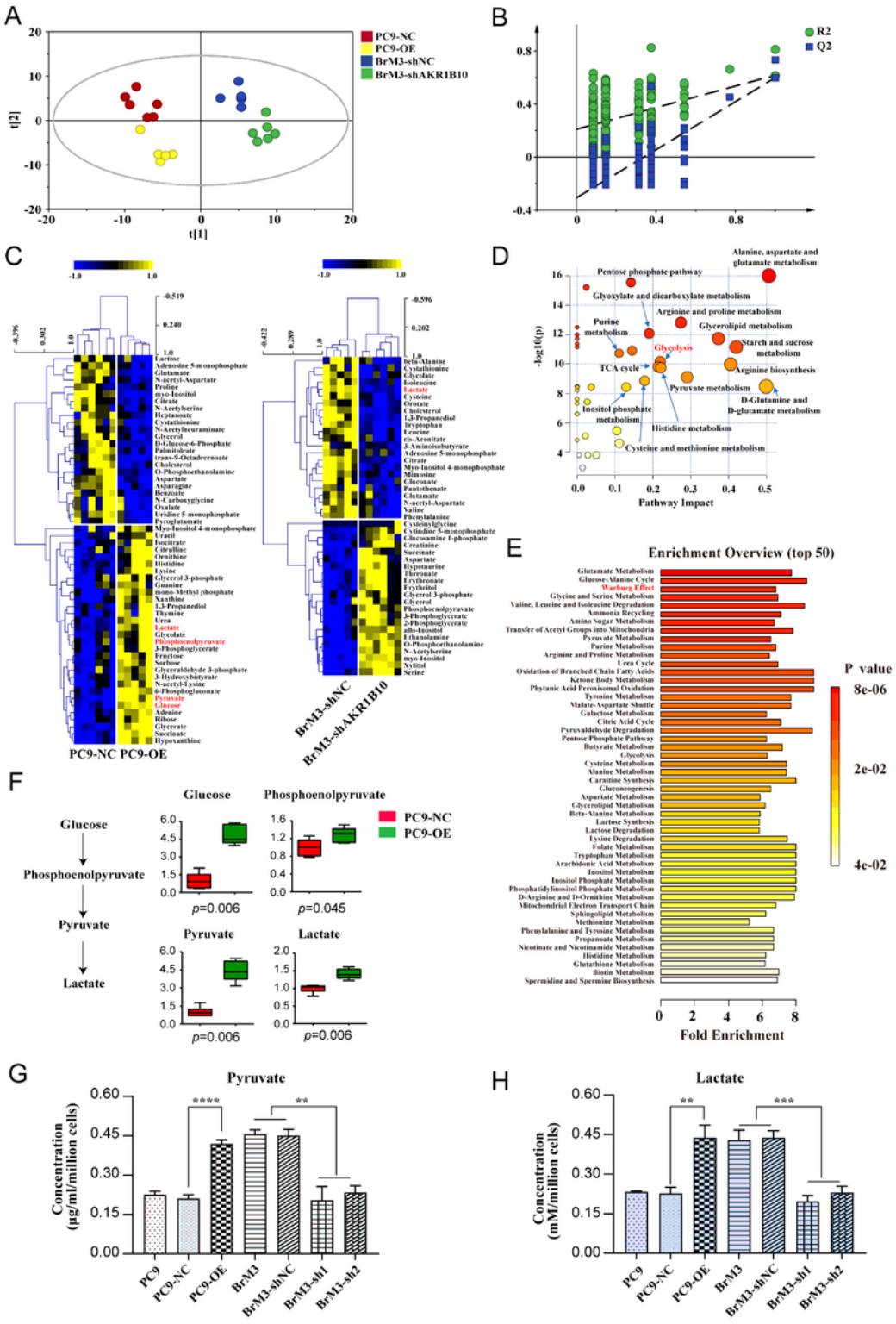

Figure 3

Metabolic profiling revealed that AKR1B10 significantly augmented the Warburg effect. (A) The PLS-DA score scatter plot with UV scaling. (B) The validation plot of permutation test with 200 cycles. (C) Heat map of focused differential annotated metabolites either in PC9-OE cells compared with PC9-NC cells, or in BrM3- shAKR1B10 cells compared with BrM3-shNC cells. (D-E) The differential metabolic pathway (D) and enriched KEGG pathways (E) in PC9-OE cells compared with PC9-NC cells. (F) The fold changes of

glucose, phosphoenolpyruvate, pyruvate and lactate in PC9-OE cells compared with PC9-NC cells. (G-H) Cellular concentrations of pyruvate (G) and lactate (H) in indicted groups. (n=3, **p<0.01, ***p<0.001, ****p<0.0001, PC9-NC, PC9 transfected with negative control plasmid; PC9-OE, PC9 transfected with AKR1B10 plasmid. shNC, PC9-BrM3 cells transfected with negative control shRNA; sh1, PC9-BrM3 cells transfected with AKR1B10-targeted shRNA vector 1; sh2, PC9-BrM3 cells transfected with AKR1B10-targeted shRNA vector 2; shAKR1B10, PC9-BrM3 cells transfected with AKR1B10-targeted shRNA vector 1)

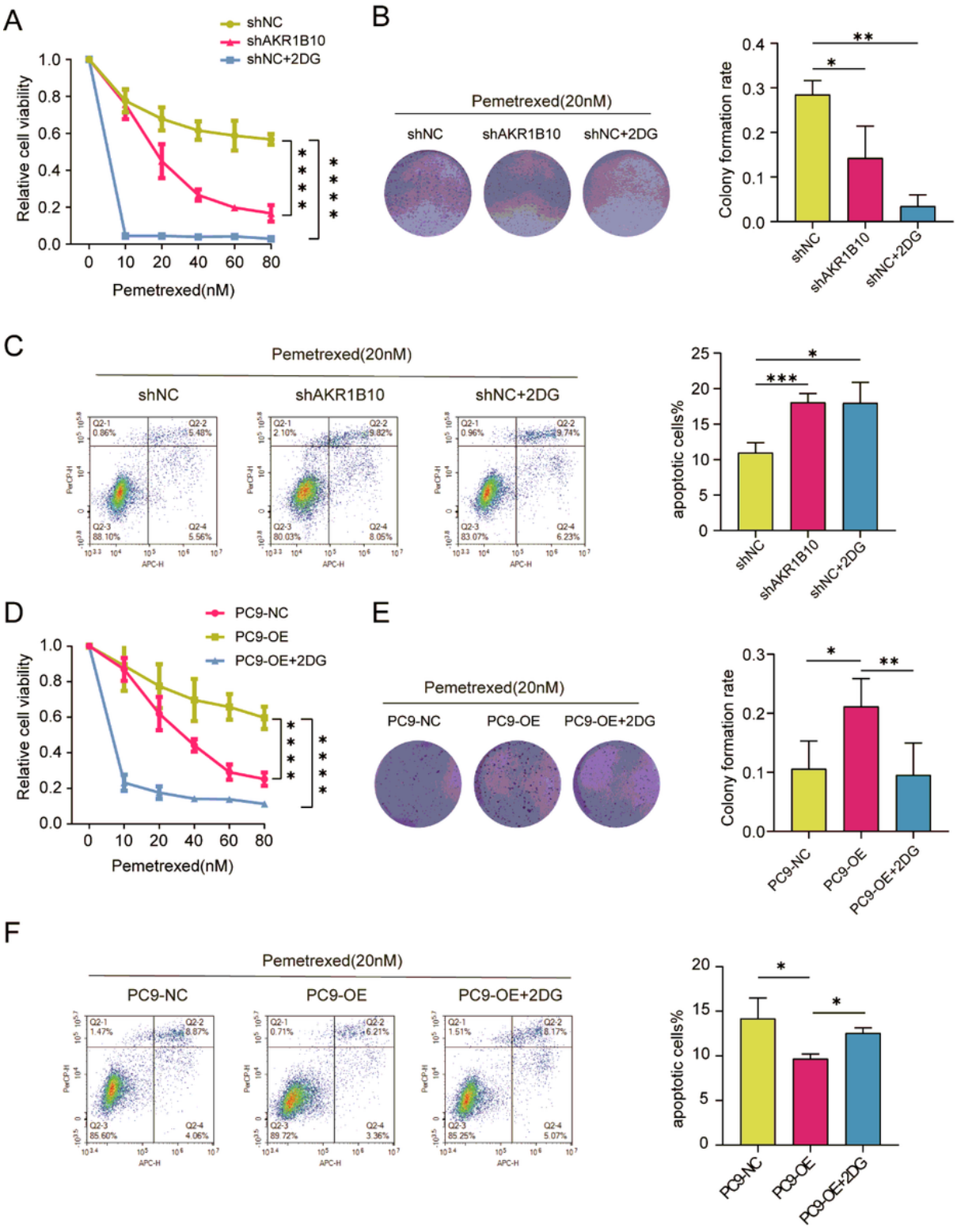

Figure 4

AKR1B10-mediated PEM resistance is dependent on the enhanced effects on anaerobic glycolysis. (A,D) Indicated cells were treated with different doses of PEM with or without 2-DG (2.5mM) for 72 h and CCK-8 assays were performed to determine their viability. (B,E) Results of clonogenic assays showing cell survival of the indicated cells after treatment with PEM (20nM) with or without 2-DG (2.5mM). Pixel density quantification of clonogenic assays is shown as histogram. (C,F) Flow cytometry analysis of the indicated cells after treatment with PEM (20nM) with or without 2-DG (2.5mM) for 24h. (n=3, *p<0.05, **p<0.01, ****p<0.0001, PC9-NC, PC9 transfected with negative control plasmid; PC9-OE, PC9 transfected with AKR1B10 plasmid. shNC, PC9-BrM3 cells transfected with negative control shRNA; shAKR1B10, PC9-BrM3 cells transfected with AKR1B10-targeted shRNA vector 1)

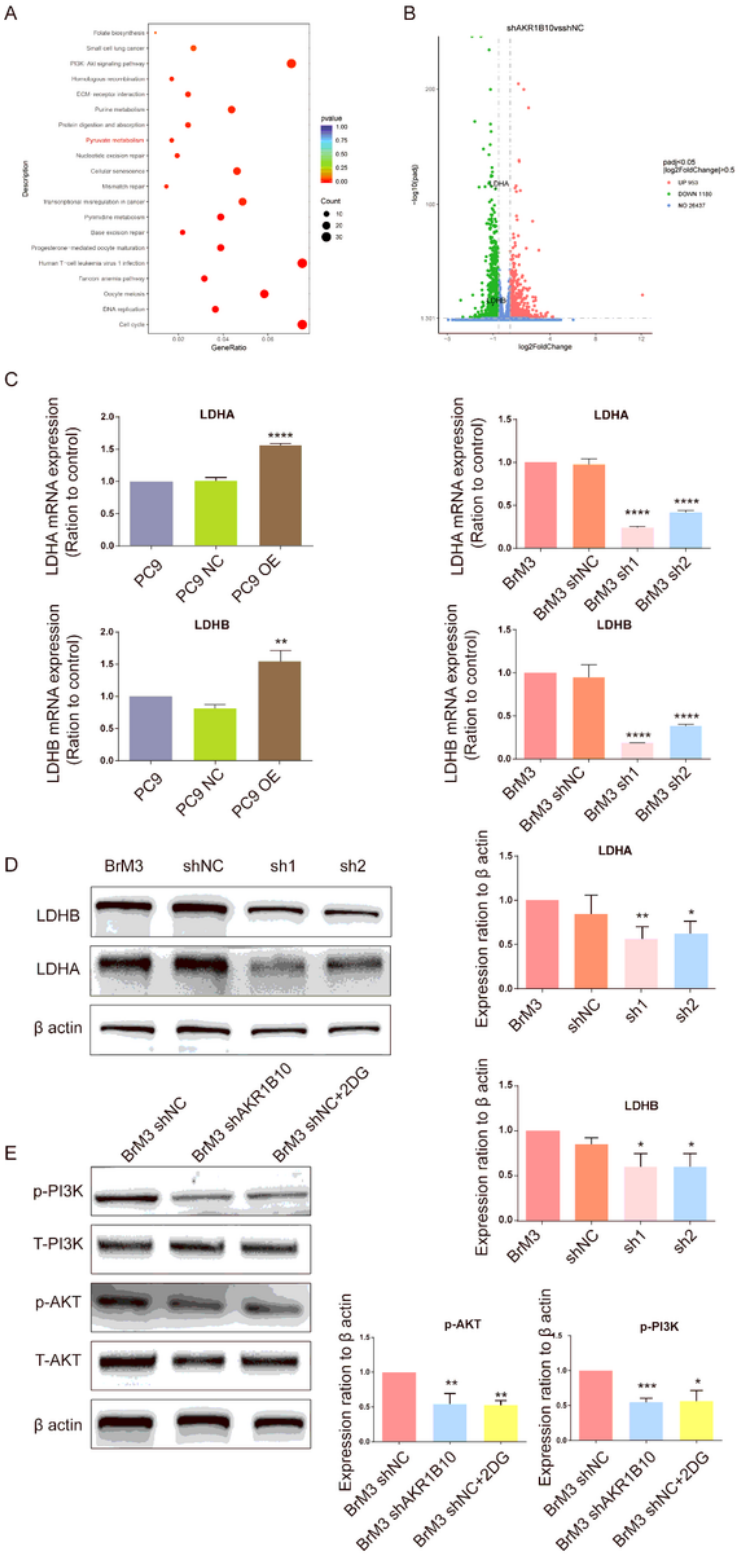

Figure 5

RNA-seq identified that AKR1B10 facilitate the Warburg metabolism by regulating the expression of glycolytic enzymes. (A) KEGG pathways enrichment analysis of downregulated differential genes. (B) Volcano plot shows the differential genes and the downregulated genes LDHA and LDHB were annotated. (C-D) The results of qPCR (C) and western blotting indicating the mRNA and protein levels of LDHA and LDHB in indicated cells. (E) The results of western blotting indicating the protein levels of PI3K pathway

in BrM3 cells, with or without AKR1B10 knockdown, or with 2-DG (2.5mM) treatment. (n=3, **p<0.01, ***p<0.001, ****p<0.0001, PC9-NC, PC9 transfected with negative control plasmid; PC9-OE, PC9 transfected with AKR1B10 plasmid. shNC, PC9-BrM3 cells transfected with negative control shRNA; sh1, PC9-BrM3 cells transfected with AKR1B10-targeted shRNA vector 1; sh2, PC9-BrM3 cells transfected with AKR1B10-targeted shRNA vector 2; shAKR1B10, PC9-BrM3 cells transfected with AKR1B10-targeted shRNA vector 1; p-PI3K, phosphorylated; T-PI3K, total PI3K; p-AKT, phosphorylated AKT; T-AKT, total AKT)

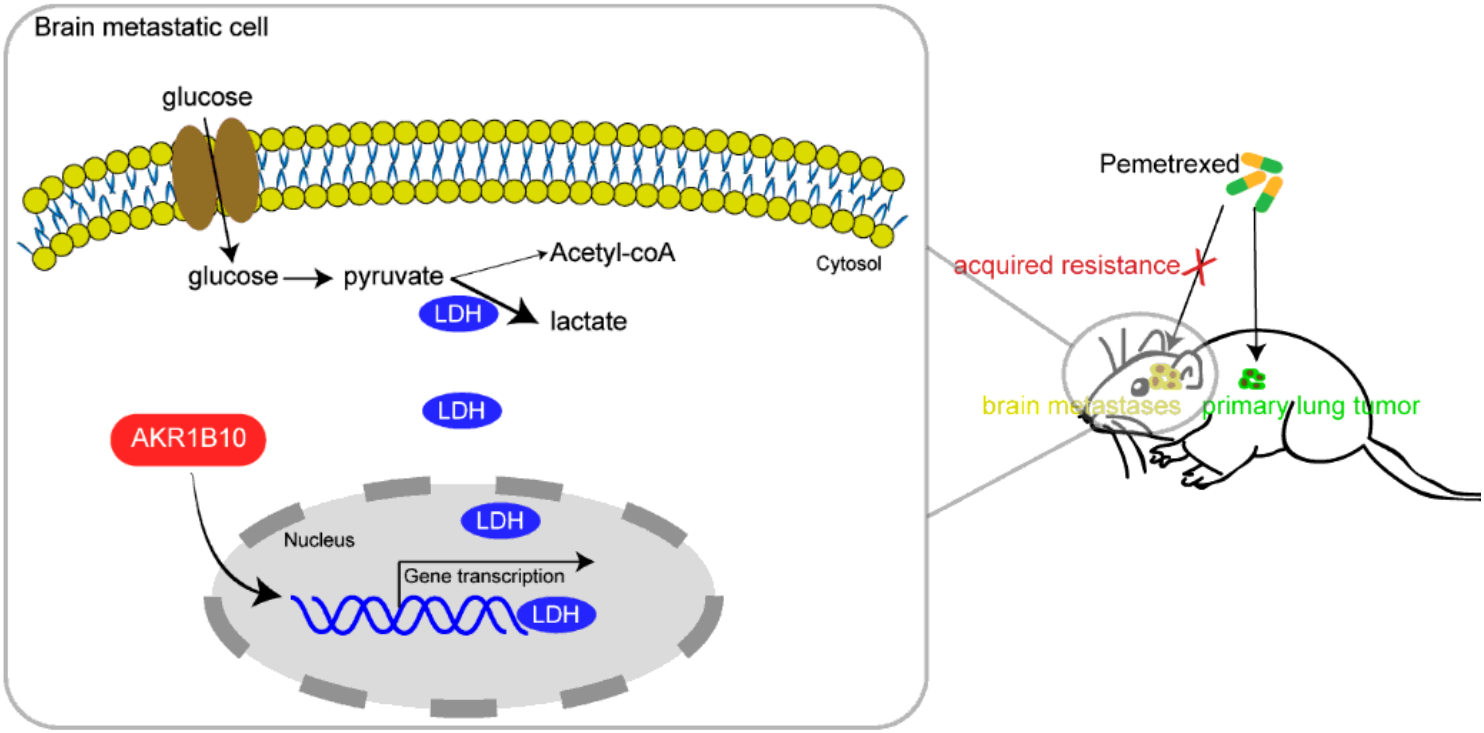

Figure 6

Illustration of the potential mechanisms by which AKR1B10 induces PEM chemotherapeutic resistance in lung cancer brain metastasis. In brain metastatic lung cancer cells, elevated AKR1B10 promotes glycolysis through activating the transcription of lactate dehydrogenases, leading to the chemotherapeutic resistance to PEM.

Supplementary Files

This is a list of supplementary files associated with this preprint. Click to download.

- TableS1.xlsx
- Supplementarymaterials.docx